Ferroelectrics

ISSN: (Print) (Online) Journal homepage: https://www.tandfonline.com/loi/gfer20

Analysis of the specific heat and the free energy and calculation of the entropy and the internal energy of $[N(CH_3)_4]_2MnBr_4$ close to the phase transition

A. Kiraci

To cite this article: A. Kiraci (2021) Analysis of the specific heat and the free energy and calculation of the entropy and the internal energy of $[N(CH_3)_4]_2MnBr_4$ close to the phase transition, Ferroelectrics, 583:1, 1-11, DOI: 10.1080/00150193.2021.1980335

To link to this article: https://doi.org/10.1080/00150193.2021.1980335

Published online: 26 Nov 2021.

FERROELECTRICS
2021, VOL. 583, 1–11
https://doi.org/10.1080/00150193.2021.1980335

Taylor & Francis
Taylor & Francis Group

Analysis of the specific heat and the free energy and calculation of the entropy and the internal energy of $[N(CH_3)_4]_2MnBr_4$ close to the phase transition

A. Kiraci

Inter-Curricular Courses Department, Cankaya University, Ankara, Turkey

ABSTRACT

The critical behavior of the specific heat and the Gibbs free energy of $[N(CH_3)_4]_2MnBr_4$ was analyzed using the Ising model close to the phase transition temperature of $T_C = 276.5$ K. Obtained value of $\alpha = 0.02$ from the Gibbs free energy and from the specific heat approximately 2.0 K and 1.4 K, respectively, below T_C (ferroelastic phase) and also deduced value of $\alpha = 0.04$ from the specific heat approximately 0.3 K above T_C (paraelastic phase) can be compared with that predicted from mean field theory ($\alpha = 0$). Also, the entropy and the internal energy of this crystal were predicted.

ARTICLE HISTORY
Received 11 February 2021
Accepted 28 June 2021

KEYWORDS
Ising model; specific heat; free energy; entropy; $[N(CH_3)_4]_2ZnBr_4$

1. Introduction

Hybrid inorganic-organic perovskites with a general chemical formula A_2BX_4 undergo reversible dielectric phase transitions are very attractive class of smart materials due to their wide applications in signal sensing, data storage and data communications [1]. A denotes the tetramethylammonium group ($N(CH_3)_4$ or shortly TMA), B is the transition metal such as Co, Cu, Zn or Mn and X represents the halogen such as Br or Cl. These materials have also reported to be a promising class of materials for optoelectronic applications. Especially, their solar cells have achieved power conversion efficiencies above % 20 [2]. This high performance of these materials are coming from the high charge carrier mobilities, high absorption coefficients, direct and tunable band gaps, a balanced electron and hole transport and long carrier diffusion lengths, as stated previously [3–6]. As a member of this family, tetramethylammonium tetrabromomanganete $[N(CH_3)_4]_2MnBr_4$ (hereafter TMA-$MnBr_4$) undergoes a second order transition from paraelastic (phase I) to ferroelastic (phase II) at around $T_C = 276.5$ K [7]. TMA-$MnBr_4$ belongs to monoclinic structure with the space group $P12_1/c1$ below the transition temperature (ferroelastic phase) and the lattice parameters in this structure is $a = 9.236$ Å, $b = 15.983$ Å, $c = 12.641$ Å and the monoclinic angle $\beta = 90.26°$ [8]. It is also reported that two kinds of chains composed of $MnBr_4$ and TMA characterize the structure in the ferroelastic phase [8]. Above the transition temperature (paraelastic phase), TMA-$MnBr_4$ belongs to orthorhombic structure with the space group Pmcn and the lattice parameters are reported to be $a = 9.301$Å, $b = 16.182$ Å and $c = 12.750$ Å [9]. In the

CONTACT A. Kiraci akiraci@cankaya.edu.tr

paraelastic phase, one kind of $MnBr_4$ molecula and two inequivalent kinds of TMA molecule are all disordered symmetrically with the mirror planes of Pmcn space group, as stated previously [9].

The phase transition mechanism of TMA-$MnBr_4$ has been studied by means of various experimental techniques. The structure of TMA-$MnBr_4$ in its low-temperature (ferroelestic) and at room temperature (paraelastic) has been reported by Hasabe and Asahi [8, 9] by means of X-ray diffraction experiments. In their X-ray diffraction study, Asahi and Hasebe [10] have measured the monoclinic angle β of TMA-XBr_4 (where X = Mn, Co, Zn and Cd) below the phase transition temperatures of these crystals and they observed an anomalous behavior of the deviation angle $\Delta\beta = \beta - 90^\circ$ for all crystals studied. The deviation angle $\Delta\beta$ increased rapidly in the paraelectric phases up to the phase transition temperature, as the temperature decreased $\Delta\beta$ decreased almost linearly and below a characteristic temperature T_0 (at which $\Delta\beta$ is presumed to be zero) $\Delta\beta$ changed it sign [10]. The dielectric measurements of TMA-$MnBr_4$ have been reported by Tanaka and Sawada [11]. In his study, Gesi [7] has showed the linear dependence between the hydrostatic pressure and the transition temperature. The luminescence properties of pure and Cu^{2+} doped TMA-$MnBr_4$ crystals have been declared by Lucas and Rodriguez [12] in their lifetime measurements and polarized optical absorption spectroscopy experiment. Zapart *et al.* [13] have declared the electron paramagnetic resonance (EPR) spectra of Mn^{2+} ions with decreasing temperature close to the phase transition temperature of TMA-$MnBr_4$. The thermoelastic properties of TMA-$MnBr_4$ were reported by Lopez-Echarri *et al.* [14] and the specific heat measurements of this crystal have been given by Ruiz-Larrea *et al.* [15].

Two different approaches by Sawada *et al.* [6–18] and by Harada [19], respectively have been suggested to explain the anomalous behavior of the deviation angle $\Delta\beta$ in TMA groups. The former one proposed a single sublattice model while the latter one proposed a coupling term between the order parameter and shear strains on the basis of the Landau type free energy. Recently, I have showed [20] that the chemical shift $\Delta\omega$ of $N_2(CH_3)_4$ ion, that is the one of the two chemically inequivalent twin structure of $N(CH_3)_4$, exhibits the similar anomalous behavior of $\Delta\beta$ in TMA-$ZnBr_4$. So, I have interpreted the phase transition mechanism of TMA-$ZnBr_4$ by relating $\Delta\omega$ (or $\Delta\beta$) to the order parameter within the framework of the dynamic Ising model [20].

Based on the theoretical models, the nature of the phase transition can be interpreted by analyzing the critical behavior of some thermodynamic quantities such as the specific heat, thermal conductivity and thermal expansion close to the phase transition temperature. A simplified lattice model of ferromagnetism (Ising model) has been applied to a variety of systems such as alloys, polymers, human brain, biological membranes and ferroelectric materials. Ising model predicts the critical behavior of the specific heat in the vicinity of the phase transition temperature, as we reported in our previous studies [21–23]. In this study, a power-law formula deduced from the Ising model was used to analyze the critical behavior of the observed [15] specific heat and Gibbs free energy data of TMA-$MnBr_4$ close to the phase transition temperature of $T_C = 276.5$ K. In addition, the entropy and the internal energy of this compound were predicted in terms of the extracted values of the critical exponent from both ferroelastic and paraelastic phases. Below in Sec. 2 the "Theory" part was given. The "Calculations and results", "Discussion" and "Conclusions" parts were given in Secs. 3, 4 and 5, respectively.

2. Theory

There are mainly two contributions to the total specific heat C_{tot} of a crystal system undergoing a phase transition which reads as

$$C_{tot} = C_{VL} + C_{VI} \tag{2.1}$$

C_{VL} is the specific heat due to the lattice contributions that is the nonsingular part, while C_{VI} is the specific heat due to the spin interactions that is the singular part of C_{tot}. The nonsingular contributions of the specific heat (C_{VL}) have been reported [24] from an Einstein (C_{VE}) and/or Debye (C_{VD}) models as

$$C_{VE} = 3Nnk[(\theta_E/T)^2 e^{\theta_E/T}/(e^{\theta_E/T} - 1)^2] \tag{2.2}$$

and

$$C_{VD} = 12\pi^4 NkT^3/5\theta_D^3 \tag{2.3}$$

where N, n and k are the number of lattice cells per mole, the number of atoms per unit cell and the Boltzmann constant, respectively while $\theta_E = h\omega_E/T$ and $\theta_D = h\omega_D/T$ are the characteristic Einstein and Debye temperatures with Einstein (Debye) characteristic frequency $\omega_E(\omega_D)$ and h is the Planck constant. Note that, Eq. (2.3) is an approximated expression which is valid at low temperatures (T^3 law). Both C_{VE} and C_{VD} (Eqs. (2.2) and (2.3)) have been derived from the lattice free energy $F_L(V,T)$ given as

$$F_L(V,T) = U_L + \frac{1}{2}\sum_i h\omega_i + kT\sum_i \ln(1 - e^{-h\omega_i/kT}) \tag{2.4}$$

where U_L is the static lattice energy and ω_i is the mode frequency.

The singular contributions of the specific heat (C_{VI}) due to the nearest neighbor spin interaction can be obtained from the Ising free energy $F_I(J(V),T)$ which reads as

$$F_I(J(V),T) = -kT\ \phi(J(V),T) \tag{2.5}$$

where $\phi(J(V),T)$ is the natural logarithm of the partition function $Z = \sum_{i,j} e^{-H_I/kT}$, while $J(V)$ represents the interaction parameter that depends on the volume of the crystal. Appearing in the partition function H_I is the Ising Hamiltonian given by

$$H_I = -J(V)\sum_{i,j}\sigma_i\sigma_j \tag{2.6}$$

where σ_i and σ_j are the Ising spin variables. It is reported that [25] critical behavior of the Ising free energy F_I in the vicinity of the phase transition temperature T_C can be written in terms of a power-law formula (compressible Ising model) according to

$$F_I = A_0' + A'|\epsilon|^{2-\alpha} \tag{2.7}$$

where $A_0' = JA_0$ and $A' = JA$ are the parameters in the dimensions of energy with constants A_0 and A, α is the critical exponent and $\varepsilon = |T - T_C|/T_C$ is the reduced temperature. From Eqs. (2.5) and (2.7), one gets

$$\phi(J(V),T) = -\frac{J}{kT}\left[A_0 + A|\epsilon|^{2-\alpha}\right] \tag{2.8}$$

The anomalous behavior of the specific heat C_{VI} can be calculated from Eq. (2.8)

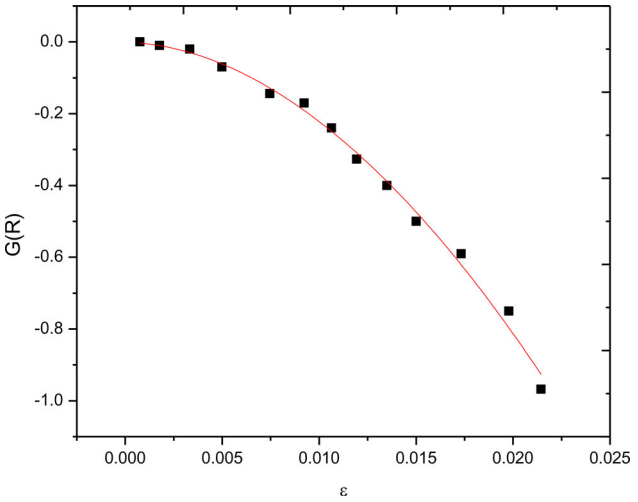

Figure 1. Gibbs free energy [15], *G*, as a function of reduced temperature ε according to Eq. (2.7) in the ferroelastic phase ($T < T_C$) of TMA-$MnBr_4$ for the temperature interval of $270.1 < T(K) < 275.8$. The solid line is guide to the eye ($T_C = 276.5$ K).

according to the thermodynamic equation which reads as

$$C_{VI} = k(J/kT)^2 \ddot{\phi} \tag{2.9}$$

where $\ddot{\phi}$ is the second derivative of ϕ (Eq. (2.8)) with respect to its argument J/kT given as

$$\ddot{\phi} = \frac{-kT^2}{JT_C}(2-\alpha)\left[(A-1)|\epsilon|^{1-\alpha} + \frac{AT}{T_C}(1-\alpha)|\epsilon|^{-\alpha}\right] \tag{2.10}$$

By neglecting the weakly divergent $|\epsilon|^{1-\alpha}$ term of Eq. (2.10), an approximated analytical expression for C_{VI} has been obtained [26] by combining Eqs. (2.9) and (2.10) which reads as

$$C_{VI} = -\frac{A'T}{T_C^2}(1-\alpha)(2-\alpha)|\epsilon|^{-\alpha} \tag{2.11}$$

The critical behavior of the entropy change ΔS and also the internal energy change ΔU can be predicted close to the transition temperature from the basic definitions of $C_V = T(\partial S/\partial T)_V$ and $C_V = (\partial U/\partial T)_V$. Inserting Eq. (2.11) into these definitions and integrating both sides, one gets

$$\Delta S = S - S_0 = -A'\frac{(2-\alpha)}{T_C}\left|\frac{T-T_C}{T_C}\right|^{1-\alpha} \tag{2.12}$$

and

$$\Delta U = U - U_0 = -A'\left[(1-\alpha)\left|\frac{T-T_C}{T_C}\right|^{2-\alpha} + (2-\alpha)\left|\frac{T-T_C}{T_C}\right|^{1-\alpha}\right] \tag{2.13}$$

where S_0 and U_0 are the entropy and the internal energy at $T = T_C$, respectively.

Table 1. Values of the A_0', A' and critical exponent α according to Eq. (2.7) in the ferroelastic phase ($T < T_C$) of TMA-$MnBr_4$ ($T_C = 276.5$ K) for the temperature intervals indicated.

$-A_0' \times 10^{-3}$ (J/mol)	$-A' \times 10^3$(J/mol)	α	Temperature interval (K)	ΔT (K)
14.2 ± 56.0	20.8 ± 32.0	0.01 ± 0.32	273.9 < T < 275.8	1.9
12.7 ± 97.3	14.3 ± 16.9	0.06 ± 0.27	278.6 < T < 275.8	3.1
14.5 ± 130.5	10.6 ± 4.5	0.12 ± 0.11	280.1 < T < 275.8	5.7
5.4 ± 109.7	9.4 ± 2.2	0.15 ± 0.06	281.5 < T < 275.8	7.1
58.0 ± 198.4	8.7 ± 2.3	0.17 ± 0.08	282.9 < T < 275.8	8.7
100.2 ± 181.1	7.8 ± 1.4	0.21 ± 0.06	284.2 < T < 275.8	9.9

3. Calculations and results

3.1. Analysis of the Gibbs free energy and the specific heat

The observed [15] Gibbs free energy data of TMA-$MnBr_4$ was analyzed according to Eq. (2.7) below ($T < T_C$) the phase transition temperature of $T_C = 276.5$ K, as given in Fig. 1. The fitting parameters A_0' and A' and also the critical exponent α were deduced for various temperature intervals, as given in Table 1. Also, the observed [15] specific heat data of this crystal were analyzed according to Eq. (2.11) in both ferroelastic ($T < T_C$) and paraelastic ($T > T_C$) phases of TMA-$MnBr_4$. The log-log graph of Eq. (2.11) was given in Fig. 2 that allows us to extract the interaction parameter A' and the critical exponent α from the intercept point and from the slope, respectively, for various temperature intervals, as indicated in Table 2. The extracted values of the critical exponent α from the Gibbs free energy (Eq. (2.7)) and also from the specific heat (Eq. (2.11)) were given in Fig. 3 as a function of change in temperature (ΔT) according to the temperature intervals indicated in Tables 1 and 2. In addition, the interaction parameter A' extracted from the Gibbs free energy (Eq. (2.7)) in the ferroelastic phase ($T < T_C$) and extracted from the specific heat (Eq. (2.11)) in both ferroelastic ($T < T_C$) and paraelastic ($T > T_C$) phases of TMA-$MnBr_4$ was given in Fig. 4 as a function of ΔT (Tables 1 and 2).

3.2. Prediction of the entropy and the internal energy

The entropy change ΔS and also the internal energy change ΔU of TMA-$MnBr_4$ were predicted in terms of Eqs. (2.12) and (2.13), respectively, as given in Figs. 5 and 6. For this prediction of ΔS and ΔU, the extracted values of the critical exponent α and the interaction parameter A' from the specific heat data (Table 2) in both ferroelastic and paraelastic phases of this compound were used.

4. Discussion

Analysis of the critical behavior of some thermodynamic functions such as the free energy and the specific heat of ferroelastic materials close to their phase transition temperatures can give some clues regarding the nature of the phase transition based on theoretical models. For this purpose, the observed [15] Gibbs free energy data of TMA-$MnBr_4$ were analyzed according to Eq. (2.7) at various temperature intervals close to the phase transition temperature of $T_C = 276.5$ K and the critical exponent α as well as the fitting parameters A_0' and A' were deduced, as given in Table 1. The obtained values

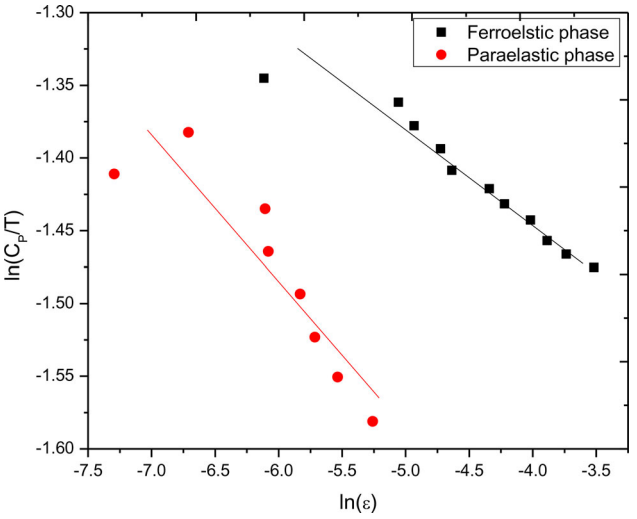

Figure 2. Specific heat [15], C_P, as a function of reduced temperature ε in a ln-ln scale according to Eq. (2.11) for the temperature intervals of $268.2 < T(K) < 275.8$ (ferroelastic phase) and $276.8 < T(K) < 277.9$ (paraelectric phase) in TMA-$MnBr_4$. The solid lines are guide to the eye.

Table 2. Values of the A' and critical exponent α according to Eq. (2.11) in both ferroelastic ($T < T_C$) and paraelastic ($T > T_C$) phases of TMA-$MnBr_4$ ($T_C = 276.5$ K) for the temperature intervals indicated.

Phase	$-A' \times 10^3$ (J/mol)	α	Temperature interval (K)	ΔT (K)
Ferroelastic	8.9 ± 0.5	0.022 ± 0.010	274.4 < T < 275.8	1.4
(T < T_C)	8.4 ± 0.5	0.037 ± 0.011	273.8 < T < 275.8	2.0
	8.3 ± 0.4	0.042 ± 0.009	272.9 < T < 275.8	2.9
	7.8 ± 0.2	0.056 ± 0.005	268.2 < T < 275.8	7.6
	7.8 ± 0.2	0.058 ± 0.005	267.1 < T < 275.8	8.7
	7.8 ± 0.1	0.059 ± 0.004	265.9 < T < 275.8	9.9
Paraelastic	7.5 ± 1.4	0.040 ± 0.032	276.8 < T < 277.1	0.3
(T > T_C)	6.4 ± 0.9	0.072 ± 0.028	276.8 < T < 277.4	0.6
	5.7 ± 0.6	0.094 ± 0.019	276.8 < T < 277.9	1.1
	5.0 ± 0.4	0.114 ± 0.014	276.8 < T < 278.6	1.8
	5.2 ± 0.3	0.112 ± 0.011	276.8 < T < 280.1	3.3
	5.4 ± 0.2	0.105 ± 0.010	276.8 < T < 281.2	4.4

of α indicated in Table 1 decreases from 0.21 to 0.02 as the change in temperature ΔT decreases from 9.9 K to 1.9 K. Note that the error parts of α increases from 0.06 to 0.37 as ΔT decreases from 9.9 K to 1.9 K. Although the deduced value of 0.02 for α is so close to that predicted from the mean field theory ($\alpha = 0$), it is reasonable to argue that extracted values of α are comparable with that predicted from the 2-d potts model ($\alpha = 0.3$) when taking into account the error parts, as we reported in our previous work for the isomorph TMA-$ZnBr_4$ [22]. Figure 1 shows the fitting procedure of Eq. (2.7) for a temperature interval of $270.1 < T(K) < 275.8$, as an example.

The structural phase transition in TMA-$MnBr_4$, as well as the other members of this family, is associated with the ordering process of the TMA groups, as stated before [15]. So, the anomalous behavior of the specific heat (C_{VI}), which was considered due to the interactions between the TMA groups in TMA-$MnBr_4$, was analyzed in terms of the compressible Ising model (Eq. (2.11)) in the vicinity of the phase transition temperature

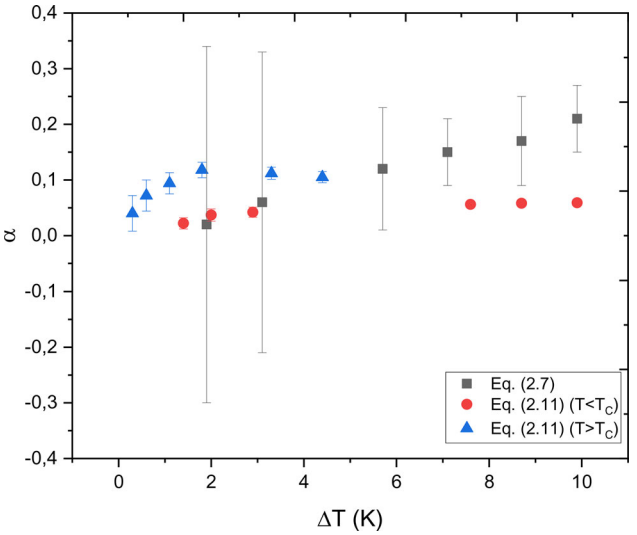

Figure 3. Values of the critical exponent α as a function of temperature Δ T (Tables 1 and 2) calculated from the Gibbs free energy [15] in the ferroelastic phase ($T < T_C$) and from the specific heat data [15] in both ferroelastic ($T < T_C$) and paraelastic ($T > T_C$) phases of TMA-$MnBr_4$ according to Eqs. (2.7) and (2.11), respectively.

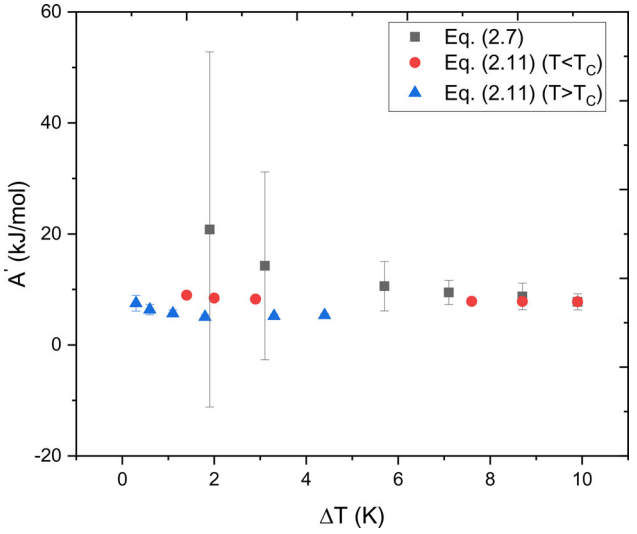

Figure 4. The fitting parameter A' deduced, independently, according to Eqs. (2.7) and (2.11) in the ferroelastic ($T < T_C$) phase of TMA-$MnBr_4$ ($T_C = 276.5$ K).

of $T_C = 276.5$ K. For this purpose, the fitting parameters A' and the critical exponent α were deduced from the reported [15] data of specific heat for TMA-$MnBr_4$ according to Eq. (2.11) in both ferroelastic ($T < T_C$) and paraelastic ($T > T_C$) phases as given in Table 2. The obtained values of α in the ferroelastic phase from 265.9 K to 275.8 K for various temperature intervals (Table 2) are decreasing from 0.06 to 0.02 as ΔT decreases from 9.9 K to 1.4 K, while the extracted values of α in the paraelastic phase from 276.8 K to 281.2 K for various temperature intervals (Table 2) are decreasing from 0.11

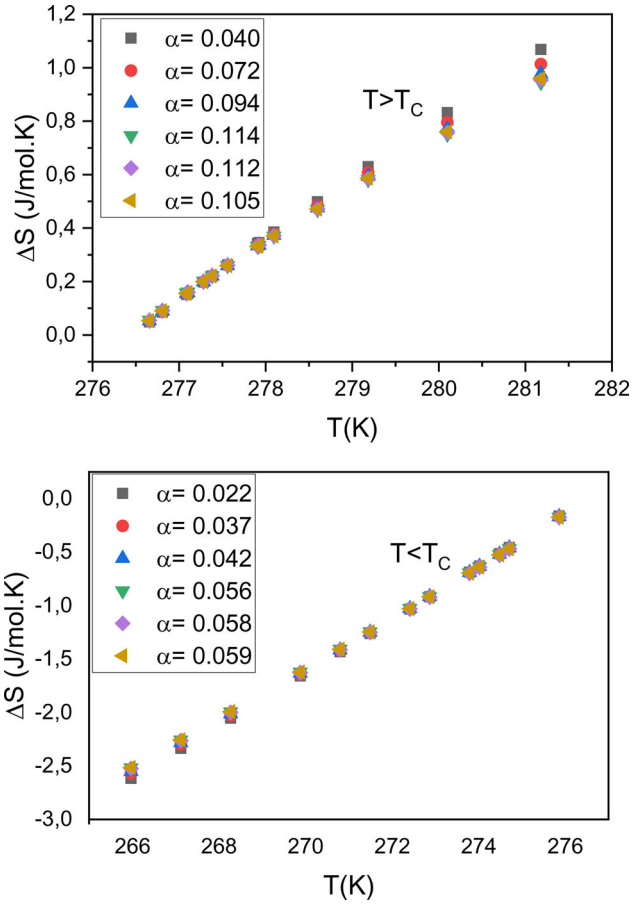

Figure 5. The entropy difference Δ S as a function of temperature according to Eq. (2.12) in both ferroelastic ($T < T_C$) and paraelastic ($T > T_C$) phases of TMA-$MnBr_4$ ($T_C = 276.5$ K).

to 0.04 as ΔT decreases from 4.4 K to 0.3 K. Our values of α 0.06 and 0.11 in ferooelastic and paraelastic phases, respectively are so close to that predicted from the 3-d Ising model ($\alpha = 1/16 = 0.07$, in ferroelastic phase, and $\alpha = 1/8 = 0.13$, in paraelastic phase). Note that, the critical exponent α calculated from both ferroelastic ($T < T_C$) and paraelastic ($T > T_C$) phases tends to decrease toward zero as temperature get closer to the transition temperature of $T_C = 276.5$ K, as predicted from the mean field theory. Our extracted values of the critical exponent from ferroelastic phase of TMA-$MnBr_4$ (Table 2) can be compared with that reported value of $\alpha = 0.01$ in the ferroelastic pahase of TMA-$CuBr_4$ [27], and also with that reported for TMA-$ZnBr_4$ [22]. Our results indicate that the Ising model studied here is adequate to describe the ferroelastic-paraelastic phase transition in TMA-$MnBr_4$. Figure 2 shows the log-log graph of Eq. (2.11) for the crystal studied here in a temperature interval of $268.2 < T(K) < 275.8$ (ferroelastic phase) and in a temperature interval of $276.8 < T(K) < 277.9$ (paraelastic phase), as examples. Those extracted values of the critical exponent α from the Gibbs free energy (Table 1) and from the specific heat (Table 2) were given in Fig. 3, for comparison, as a function of ΔT. Also, those extracted values of the interaction parameter A' according to Eqs. (2.7) and (2.11), independently, were given in Fig. 4 as a function of temperature.

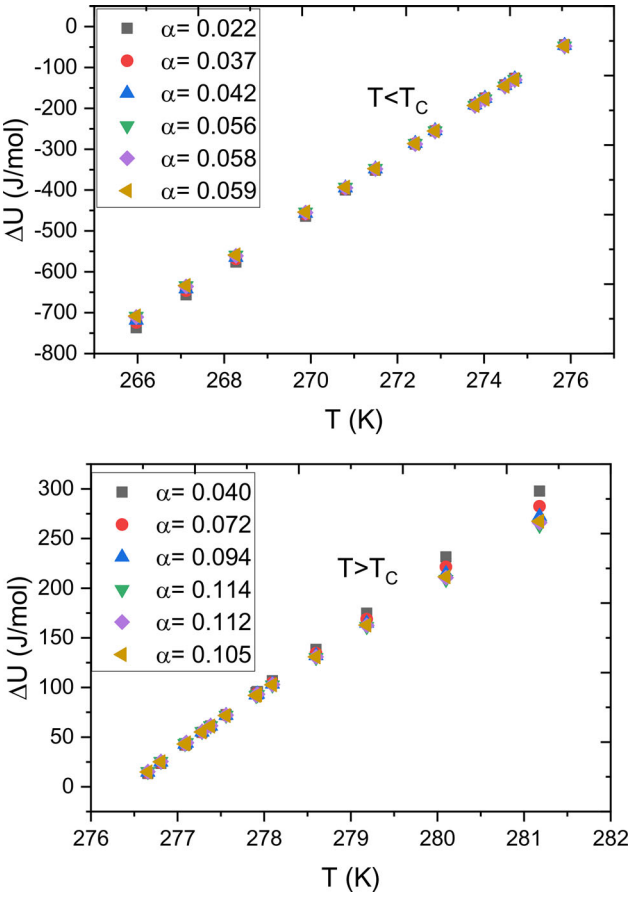

Figure 6. The enthalpy difference Δ H as a function of temperature according to Eq. (2.13) in both ferroelastic ($T < T_C$) and paraelastic ($T > T_C$) phases of TMA-$MnBr_4$ ($T_C = 276.5$ K).

Regarding the analysis of the nonsingular part of the total specific heat, C_{VL}, Einstein and/or Debye models (Eqs. (2.2) and (2.3)) can be used if enough spectroscopic information about the phonon spectrum is known. We have found no available phonon spectrum data for TMA-$MnBr_4$ in the literature to do this calculation. Such a calculation has been performed for the isomorph TMA-$ZnBr_4$ [28]. The contribution of the external modes in TMA-$ZnBr_4$ have been calculated with a unique Debye frequency of $\omega_D = 56\,\mathrm{cm}^{-1}$ by using the Raman spectra in the frequency range 0 and $60\,\mathrm{cm}^{-1}$, as reported before [28].

Once we deduced the values of the interaction parameter A' and the critical exponent α from the observed [15] specific heat data in both phases of TMA-$MnBr_4$ (Table 2), we were able to predict the entropy change ΔS and the internal energy change ΔU close to the phase transition temperature $T_C = 276.5$ K according to Eqs. (2.12) and (2.13), respectively. The temperature dependence of ΔS and ΔU is given in Figs. 5 and 6, respectively.

5. Conclusions

The phase transition mechanism of TMA-$MnBr_4$ was investigated by means of power-law formulas deduced from the Ising model close to the phase transition temperature of

276.5 K. The values of 0.02 and 0.04 for the critical exponent were extracted from the observed specific heat data as the phase transition temperature is approached from below and above, respectively. Both values are very close to that predicted from the mean field theory. This is an indication of that Ising model studied here explains well the second order ferroelastic-paraelastic phase transition of TMA-$MnBr_4$. In addition, the calculation of the entropy and the internal energy was performed using the critical exponent extracted from the observed specific heat data of TMA-$MnBr_4$ close to the phase transition temperature of 276.5 K.

References

[1] S. Chai *et al.*, Dielectric phase transition of an A2BX4-type perovskite with a pentahedral to octahedral transformation, *Dalton Trans.* **49** (7), 2218 (2020). DOI: 10.1039/c9dt04270a.

[2] S. Brittman, G. W. P. Adhyaksa, and E. C. Garnett, The expanding world of hybrid perovskites: materials properties and emerging applications, *MRS Commun.* **5** (1), 7 (2015). DOI: 10.1557/mrc.2015.6.

[3] J. H. Noh *et al.*, Chemical management for colorful, efficient, and stable inorganic-organic hybrid nanostructured solar cells, *Nano Lett.* **13** (4), 1764 (2013). DOI: 10.1021/nl40034b.

[4] S. D. Stranks *et al.*, Electron-hole diffusion lengths exceeding 1 micrometer in an organometal trihalide perovskite absorber, *Science* **342** (6156), 341 (2013). DOI: 10.1126/science.1243982.

[5] Q. Dong *et al.*, Solar cells. Electron-hole diffusion lengths $> 175\,\mu$m in solution-grown $CH_3NH_3PbI_3$ single crystals, *Science* **347** (6225), 967 (2015). DOI: 10.1126/science.aaa5760.

[6] D. Shi *et al.*, Solar cells. Low trap-state density and long carrier diffusion in organolead trihalide perovskite single crystals, *Science* **347** (6221), 519 (2015). DOI: 10.1126/science.aaa2725.

[7] K. Gesi, Phase transition in $\{N(CH_3)_4\}_2$ $MnBr_4$, *J. Phys. Soc. Jpn.* **52** (8), 2931 (1983). DOI: 10.1143/JPSJ.52.2931.

[8] K. Hasebe, T. Asahi, and K. Gesi, Structure of tetramethylammonium tetrabromomanganate in its low-temperature phase, *Acta Crystallogr. C Cryst. Struct. Commun.* **46** (5), 759 (1990). DOI: 10.1107/S0108270189009704.

[9] K. Hasebe and T. Asahi, Structure of tetramethylammonium tetrabromomanganate at room temperature, *Acta Crystallogr. C Cryst. Struct. Commun.* **45** (6), 841 (1989). DOI: 10.1107/S0108270188013976.

[10] T. Asahi and K. Hasebe, Measurement of monoclinic angle in the ferroelastic phase of $[N(CH_3)_4]_2$ XBr_4 (X = Zn, Co, Mn, Cd), *J. Phys. Soc. Jpn.* **63** (7), 2827 (1994). DOI: 10.1143/JPSJ.63.2827.

[11] K. Tanaka and A. Sawada, Dielectric study of ferridistortive phase transition in $[N(CH_3)_4]_2$ $MnBr_4$ crystals, *Ferroelectrics* **159** (1), 221 (1994). DOI: 10.1080/00150199408007576.

[12] M. C. M. Lucas and F. Rodriguez, Luminescence properties of Cu^{2+} doped TMA_2MnBr_4 crystals and a spectroscopic study of the $CuBr_4^{2}$ complexes formed, *J. Phys.: Cond. Matter* **5**, 2625 (1993).

[13] W. Zapart *et al.*, Phase Transition in $[N(CH_3)_4]_2MnBr_4$ by EPR, *J. Korean Phys. Soc.* **32**, 697 (1998).

[14] A. Lopez-Echarri, I. Ruiz-Larrea, and A. Fraile-Rodriguez, The thermoelastic properties of $[N(CH_3)_4]_2$ $ZnBr_4$ and $[N(CH_3)_4]_2$ $MnBr_4$, *Phase Transit* **71** (2), 101 (2000). DOI: 10.1080/01411590008224542.

[15] I. Ruiz-Larrea *et al.*, The Specific Heat of Tetramethylammonium Salts, *J. Therm. Anal. Cal.* **61** (2), 503 (2000). DOI: 10.1023/A:1010125702916.

[16] A. Sawada and K. Tanaka, Ferridistortive phase transitionin $[N(CH_3)4]_2$ $CoBr_4$ Crystals, *J. Phys. Soc. Jpn.* **60** (12), 4326 (1991). DOI: 10.1143/JPSJ.60.3593.
[17] K. Tanaka *et al.*, Roles of cation and anion molecules in ferridistortive phasetransition in $[A(CH_3)_4]_2$ XBr_4 type crystals, *J. Phys. Soc. Jpn.* **64** (1), 146 (1995). DOI: 10.1143/JPSJ.64.146.
[18] K. Gesi, Dielectric study of the structural phase transition in $[N(CH_3)_4]_2$ $CdBr_4$, *Phase Transit* **38** (1), 1 (1992). DOI: 10.1080/01411599208203455.
[19] S. Harada, M. Iwata, and Y. Ishibashi, Measurement of elastic constant in $[N(CH_3)_4]_2$ $ZnBr_4$ single crystal, *J. Phys. Soc. Jpn.* **61** (10), 3436 (1992). DOI: 10.1143/JPSJ.61.3436.
[20] A. Kiraci, The important role of $N_2(CH_3)_4$ ion in the phase-transition mechanism of $[N(CH_3)_4]_2ZnBr_4$, *IEEE Trans. Ultrason. Ferroelectr. Freq. Control.* **67** (5), 1053 (2020). DOI: 10.1109/TUFFC.2019.2962868.
[21] A. Kiraci, A phenomenological study on ferroelectric pyridinium tetrafluoroborate (C_5NH_6) BF_4, *Thermochim. Acta* **680**, 178371 (2019). DOI: 10.1016/j.tca.2019.178371.
[22] A. Kiraci, Analysis of the specific heat and the free energy of $[N(CH_3)_4]_2$ $ZnBr_4$ close to the ferro-paraelastic phase transition, *Phase Transit* **92** (3), 249 (2019). DOI: 10.1080/01411594.2019.1566547.
[23] H. Yurtseven, D. V. Tirpanci, and H. Karacali, Analysis of the specific heat of Ru doped $LiKSO_4$ close to phase transitions, *High Temp.* **56** (3), 462 (2018). DOI: 10.1134/S0018151X18030239.
[24] M. Born and K. Huang, *Dynamical theory of crystal lattices* (Oxford University Press, Oxford, 1954).
[25] H. Yurtseven, Weakly first-order or nearly second-order phase transitions, *Phase Transit* **47** (1–2), 59 (1994). DOI: 10.1080/01411599408200336.
[26] H. Yurtseven and W. H. Sherman, Weakly first-order or nearly second-order phase transitions in ammonium halides, *Phase Transit* **47** (1–2), 69 (1994). DOI: 10.1080/01411599408200337.
[27] A. L. Echarri, I. R. Larrea and M. J. Tello, Thermodynamics of the phase transition sequence in the incommensurate compound $[N(CH_3)_4]_2CuBr_4$, *Phys. Stat. Sol. (B)* **154** (1), 143 (1989). DOI: 10.1002/pssb.2221540113.
[28] J. M. Igartua *et al.*, Calorimetric and Raman study of the phase transition in $[N(CH_3)_4]_2ZnBr_4$, *Phys. Stat. Sol. (B)* **168** (1), 67 (1991). DOI: 10.1002/pssb.2221680106.